Title
A modular methodology for time-domain stochastic seismic wave propagation

Authors
Wang, Fangbo
Wang, Hexiang
Yang, Han
et al.

Publication Date
2021-11-01

DOI
10.1016/j.compgeo.2021.104409

Peer reviewed

A Modular Methodology for Time-domain Stochastic Seismic Wave Propagation

Fangbo Wang[1], Hexiang Wang[2], Han Yang[2], Yuan Feng[2], and Boris Jeremić*[2,3]

[1]School of Civil Engineering, Tianjin University, Tianjin, China

[2]Department of Civil and Environmental Engineering, University of California, Davis, CA, USA

[3]Earth and Environmental Sciences Area, Lawrence Berkeley National Laboratory, Berkeley, CA, USA, Email:jeremic@ucdavis.edu

ABSTRACT

Presented here is a modular methodology for time-domain stochastic seismic wave propagation analysis. Presented methodology is designed to analyze uncertain seismic motions as an input, propagating through uncertain material. Traditional approach for uncertain wave propagation relies on models that include deep bedrock, local soil site, and their random process and random field information. Such models can become quite large and computationally intractable. The modular approach proposed herein features two step approach that allows separate consideration of the deep bedrock and local site along with corresponding random field information. The first step considers an auxiliary stochastic motions problem in the bedrock. Stochastic local site response can then be simulated in a reduced domain within certain depth from the surface. Application of uncertain seismic motions at depth, for local uncertain site response is done using stochastic effective forces developed through the Domain Reduction Method. By using Hermite polynomial chaos expansion to represent the non-Gaussian random field of material parameters and non-stationary random process of seismic motion, the proposed modular methodology is formulated using intrusive stochastic Galerkin approach, as seen in the Stochastic Elastic-Plastic Finite Element Method (SEPFEM).

Developed modular methodology is illustrated using a 1-D stochastic seismic wave propagation analysis with three cases, and simulation results are also verified with results from conventional approach.

Keywords: Stochastic seismic wave propagation   Modular methodology   Domain reduction method   Intrusive Galerkin stochastic finite element method   Hermite polynomial chaos

1 INTRODUCTION

The necessity to account for inevitable uncertainties to predicted seismic behaviour has long been recognized in the earthquake engineering community (Moehle and Deierlein 2004), nonlinear seismic wave propagation analysis rarely accounts for uncertainties. This omission of uncertain, nonlinear wave propagation analysis results largely from the significant computational burden. There are two ways to improve the computational efficiency. The first one employs effective, artificial boundary conditions close to the surface soil site of interest, in order to reduce the size of computational domain of the model while following proper physics of wave propagation in infinite media, while the second one utilizes a highly efficient stochastic method to overcome the computational burden when extended to stochastic analysis.

Significant progress has been made on development of artificial boundary for modelling wave propagation in reduced domain. Viscous boundary was first formulated by Lysmer and Kuhlemeyer (1969) for 1D wave propagation, where effective shear stress time history is input to the base with viscous dash-pots as non-reflecting boundary. Liu et al. (2006) extended the viscous boundary to viscous-spring boundary for 3D wave propagation. Excitations from far field could be approximately input as equivalent normal and shear stress time history along the viscous-spring boundary. In addition, some global artificial boundaries, e.g., Lysmer and Waas (1972) and Kausel (1994), satisfy the radiation condition of infinite medium exactly but have complex formulations and are rarely used in practice. In the context of finite element method (FEM), Bielak et al. (2003) formulated Domain Reduction Method (DRM) that can input seismic excitations as dynamically consistent nodal forces exerted on a single layer of elements surrounding the reduced FEM model. As an effective boundary, the DRM has been successfully applied to the simulation of near field seismic response

(Yoshimura et al. 2003; Kontoe et al. 2009) and earthquake soil structure interaction (Jeremić and Preisig. 2005; Jeremić et al. 2007; Jeremić et al. 2009; Jeremić et al. 2021; Isbiliroglu et al. 2015). Although use of the DRM significantly reduces the computational burden for deterministic wave propagation problems, stochastic seismic wave propagation considering inherent uncertainties is still challenging. To the best knowledge of the authors', there is still no development on artificial boundary and reduced domain modelling technique in probabilistic context.

The most straightforward way to handle the uncertainty is Monte Carlo method. All the above artificial boundary and reduced domain modelling technique are directly applicable. Monte Carlo method essentially generates statistically significant number of samples for input uncertainties of the model, and runs deterministic solver repeatedly for all the samples (Metropolis and Ulam 1949). Results from deterministic runs are collected and analysed to obtain the statistics of response, see for example Shinozuka (1972), Fenton and Griffiths (2002), Fenton and Griffiths (2005) for applications of Monte Carlo method. However, Monte Carlo method is computationally intractable with its notoriously slow convergence rate, and requires extensive number of samples to reach satisfactory result with engineering accuracy. Alternative approaches, such as perturbation approach and stochastic collocation approach are also popular. Perturbation approach employs first order or second order Taylor expansions of random functions (Bourret 1962). Early works on stochastic seismic wave propagation through geologic media mainly rely on perturbation method (Manolis and Shaw 1996; Rahman and Yeh 1996; Zhang and Lou 2001). However, its application is limited to small uncertainties due to the utilization of only first or second order Taylor series (Sudret and Kiureghian 2000). Similar to the Monte Carlo method, stochastic collocation also repeatedly executes deterministic solver for all samples but the samples are judiciously selected by quadrature rules (Xiu and Hesthaven 2005; Babuška et al. 2007). Although the number of samples is much smaller than that of Monte Carlo method, the stochastic collocation method is still computationally expensive for high-dimensional problems because of the exponential increase of sample size in high dimensions (Xiu 2010; Berveiller et al. 2006). Note that the above-mentioned stochastic methods are not altering deterministic codes, and are all regarded as non-intrusive methods.

On the other hand, stochastic Galerkin method, which is an intrusive method and proposed by Ghanem and Spanos (1991), represents input uncertainties in polynomial functional form, e.g., Hermite polynomial chaos expansion. Galerkin projection is performed to establish a generalized expanded linear system of equations, whose solutions are the coefficients of polynomial chaos expansion of uncertain response. Although the stochastic Galerkin method requires modification/redevelopment of the deterministic program, it can be shown that intrusive stochastic Galerkin method is advantageous over non-intrusive approaches in terms of computational efficiency (Xiu 2010). Recently, a time-domain intrusive stochastic elastic-plastic finite element method was developed by Sett et al. (2011), Wang and Sett (2016) using stochastic Galerkin method. Developed methodology can incorporate non-Gaussian random field for uncertain material parameters and non-stationary random process for uncertain seismic loads, and perform stochastic seismic wave propagation analysis (Wang and Sett 2019). Due to its computational efficiency, this paper extends the conventional deterministic domain reduction method (Bielak et al. 2003) to probabilistic regime within the framework of Galerkin stochastic finite element method. Established is a two-step modular methodology for time-domain intrusive stochastic seismic wave propagation. It is expensive to perform conventional one-step stochastic seismic wave propagation in a holistic model including detailed modelling of both bedrock and local site, and their random field information. While in the proposed modular methodology, the first step considers stochastic seismic wave propagation where the bedrock is modelled in detail as a random field and the local site is only modelled as a deterministic field with coarse mesh. The second step performs stochastic nonlinear seismic wave propagation analysis in a reduced domain with detailed modelling of local random site. Connection of the two steps is a boundary layer whose response is recorded at the first step and again applied at the second step as effective stochastic earthquake forces for DRM.

Novelty of this work lies in extending the deterministic DRM into stochastic context using intrusive stochastic Galerkin formulation. The deterministic DRM is a modular methodology to reduce computational burden in seismic wave propagation analysis. The extension to stochastic context, namely, the proposed modular methodology, inherits the advantage of deterministic DRM which allows reduction of computational domain to improve simulation efficiency. Compared to the traditional approach with holistic model, the proposed modular approach benefits from separate consideration of random bedrock model and random local site model. Relatively large mesh size and time step can be adopted in the stochastic modelling of the first step, which needs to be performed only once. Only the second part of the computation needs to be repeated if any system parameters within local site need to be varied.

Formulation of the time-domain intrusive stochastic finite element method (SFEM) is first introduced in section 2. Two-step modular methodology within SFEM is established by extending conventional domain reduction method to probabilistic regime. Salient features of the proposed modular methodology are illustrated through three examples. The first example assumes the only uncertainty to be shear modulus of bedrock and local site, and models them as non-Gaussian random fields. The second example assumes the only uncertainty to be the seismic motion and models it as a non-stationary random process. The third example accounts for uncertainties in both seismic motions and material parameters. Simulation results are presented in terms of marginal mean, marginal standard deviation, marginal probabilistic density function, and compared with conventional stochastic seismic wave propagation analysis using holistic model.

2 FORMULATION OF TIME-DOMAIN INTRUSIVE STOCHASTIC FINITE ELEMENT METHOD

The weak form of deterministic, dynamic finite element method with body force neglected, can be written as (Bathe 1996):

$$\begin{aligned}\sum_e \Big[\int_{D_e} & N_m(\mathbf{x})\rho(\mathbf{x})N_n(\mathbf{x})d\Omega\ \ddot{u}_n(t) + \\ & \int_{D_e} \nabla N_m(\mathbf{x})D(\mathbf{x},t)\nabla N_n(\mathbf{x})d\Omega\ u_n(t) - \\ & \qquad \int_{D_e} N_m(\mathbf{x})f^b(\mathbf{x},t)d\Omega - f_m(\mathbf{x},t)\Big] = 0 \end{aligned} \tag{1}$$

where $\mathbf{x}$ denotes the location vector defined over the domain, $N(\mathbf{x})$ is the finite element shape function, $\rho(x)$ is the material density, $D(\mathbf{x},t)$ is the tangent stiffness which should be updated for nonlinear materials, $f^b(\mathbf{x}, t)$ is the body force and $f(\mathbf{x}, t)$ represents all other external forces(traction, point load, etc.). $\sum_e$ denotes the finite element assembly procedure over the discretized domain. The nodal displacement $u_n(t)$, nodal acceleration $\ddot{u}_n(t)$ can be solved using a time integration scheme.

To account for the uncertainties in the system, the above deterministic finite element is extended to stochastic finite element with the material parameters $D(\mathbf{x}, t)$ modelled as random fields and forcing functions $f(\mathbf{x}, t)$ modelled as random processes. Following Wang and Sett (2016), material parameters $D(\mathbf{x}, t)$ and forcing functions $f(\mathbf{x}, t)$ can be represented by a multidimensional Hermite polynomial chaos expansion (PC) with the correlation structure quantified by Karhunen-Loève theorem. Since the quantification of a random field and random process follow the same procedure, the formulation is only illustrated for the random field below.

Let $D(\mathbf{x})$ denote a heterogeneous non-Gaussian random field that can be represented by a multidimensional Hermite polynomial chaos as:

$$D(\mathbf{x}, \theta) = \sum_{i=1}^{P_1} a_i(\mathbf{x}) \Psi_i(\{\xi_r(\theta)\}) \tag{2}$$

where $\{\xi_r(\theta)\}$ denotes the set of independent zero-mean unit-variance Gaussian random variables, and $\{\Psi\}$ is the PC basis set consisting of multidimensional orthogonal Hermite polynomials, while $a_i(\mathbf{x})$ is the coefficient for PC basis Ψ_i and $\mathbf{x}$ represents the location vector within the random field. Note that θ indicates randomness, and will be dropped to simplify notation. The total number of PC terms, P_1, may be computed as $P_1 = (M_1 + p_1)!/(M_1!p_1!)$ where M_1 denotes the dimension of PC expansion, i.e., the number of Gaussian variables in $\{\xi_r\}$, and p_1 denotes the order of PC expansion.

To this end, the main task is to quantify the marginal distributions and correlation functions of the random field. We begin with the marginal distribution quantification by using a one-dimensional Hermite polynomial chaos as:

$$D(\mathbf{x},\theta) = \sum_{i=0}^{p_1} \alpha_i(\mathbf{x})\Gamma_i(\gamma(\cdot,\theta)) \tag{3}$$

where the set $\{\Gamma\}$ consists of one-dimensional Hermite polynomials up to order p_1 while the variable of polynomials is a zero-mean unit-variance Gaussian random field γ. The coefficient $\alpha_i(\mathbf{x})$ is computed by $\langle D\,\Gamma_i\rangle/\langle\Gamma_i^2\rangle$ for each location while $\langle\cdot\rangle$ denotes the ensemble operator. Note that $\langle\Gamma_i^2\rangle$ can be precomputed analytically, and $\langle D\,\Gamma_i\rangle$ can be evaluated using inverse CDF transformation technique (Xiu 2010).

In addition, the covariance function of random field $D(\mathbf{x})$ can also be derived in terms of the covariance function of $\gamma(\mathbf{x})$ (Sakamoto and Ghanem 2002) as:

$$C_D(\mathbf{x}_1,\mathbf{x}_2) = \sum_{i=1}^{p} \alpha_i(\mathbf{x}_1)\alpha_i(\mathbf{x}_2) i! C_\gamma(\mathbf{x}_1,\mathbf{x}_2)^i \tag{4}$$

After solving Eq. 4 to obtain the covariance function of $\gamma(\mathbf{x})$, $C_\gamma(\mathbf{x}_1,\mathbf{x}_2)$, Karhunen-Loève expansion is then employed to efficiently discretize the zero-mean unit-variance Gaussian random field γ. A generalized eigenvalue problem is formulated using finite element method to solve the Fredholm integral of the second kind with kernel $C_\gamma(\mathbf{x}_1,\mathbf{x}_2)$, then, random field $\gamma(\mathbf{x})$ may be written in terms of eigenvalues λ and eigenvectors $y(\mathbf{x})$:

$$\gamma(\mathbf{x},\theta) = \sum_{i=1}^{M_1} \frac{\sqrt{\lambda_i}\, y_i(\mathbf{x})}{\sqrt{\sum_{m=1}^{M_1}\left\{\sqrt{\lambda_m}\, y_m(\mathbf{x})\right\}^2}}\ \xi_i(\theta) \tag{5}$$

Note that only the first M_1 eigenvalues and eigenvectors are selected for the Karhunen-Loève expansion, and the unit variance constraint is satisfied by normalization.

Substituting Eq. 5 into Eq. 3, and equating the two representations of random field $D(\mathbf{x})$, Eq. 3 and Eq. 2, the PC coefficients $\{a_i\}$ can be found as:

$$a_i(x) = \frac{p!}{\langle\Psi_i^2\rangle}\alpha_p(x)\prod_{j=1}^{p} \frac{\sqrt{\lambda_{r_{(j)}}}\, y_{r_{(j)}}(x)}{\sqrt{\sum_{m=1}^{M_1}\left\{\sqrt{\lambda_m}\ y_m(x)\right\}^2}} \tag{6}$$

Similarly, the random forcing function can also be represented using multidimensional Hermite

PC with dimension M_2 and order p_2 as:

$$f_m(t,\theta) = \sum_{j=1}^{P_2} f_{mj}(t)\Psi_j(\{\xi_r(\theta)\}) \tag{7}$$

where $f_{mj}(t)$ is the PC coefficient at time t for random forcing, and may be computed by following the same procedure as the random field. The output response processes, $u_n(t,\theta)$, $\ddot{u}_n(t,\theta)$ can also be represented by multidimensional Hermite PC as:

$$u_n(t,\theta) = \sum_{k=1}^{P_3} d_{nk}(t)\Psi_k(\{\xi_l(\theta)\}) \tag{8}$$

$$\ddot{u}_n(t,\theta) = \sum_{k=1}^{P_3} \ddot{d}_{nk}(t)\Psi_k(\{\xi_l(\theta)\}) \tag{9}$$

where $d_{nk}(t)$, $\ddot{d}_{nk}(t)$ are the unknown PC coefficients that will be obtained through a stochastic Galerkin projection.

After substitution of Eqs. 2, 7, 8, 9 into Eq. 1 and after application of stochastic Galerkin projection by multiplying both sides with Ψ_l, and after taking expectation, one obtains:

$$\begin{aligned} &\sum_{k=1}^{P_3}\langle\Psi_k\Psi_l\rangle \sum_{n=1}^{\bar{N}} \int_{D_e} N_m(x)\rho(x)N_n(x)d\Omega \;\; \ddot{d}_{nk}(t) \;\; + \\ &\quad \sum_{k=1}^{P_3}\sum_{i=1}^{P_1}\langle\Psi_i\Psi_k\Psi_l\rangle \sum_{n=1}^{\bar{N}} \int_{D_e} \nabla N_m(\mathbf{x})a_i(x)\nabla N_n(\mathbf{x})d\Omega \;\; d_{nk}(t) = \sum_{j=1}^{P_2}\langle\Psi_j\Psi_l\rangle f_{mj}(t) \end{aligned} \tag{10}$$

where $\bar{N}$ is the total number of nodes in the deterministic finite element domain. Note that Eq. 10 is similar to the deterministic finite element formulation (Eq. 1) with additional wrapping indices about Hermite PC, consequently, the deterministic matrix assembly can be viewed as a block matrix and Eq. 10 can be assembled into a generalized matrix-vector form as:

$$M\ddot{d} + Kd = F \tag{11}$$

where $\boldsymbol{M}$ and $\boldsymbol{K}$ may be called the generalized mass and stiffness matrices, while $\boldsymbol{F}$, $\boldsymbol{d}$, and $\ddot{\boldsymbol{d}}$ may be called the generalized force, displacement, and acceleration vectors, respectively. By introducing Rayleigh damping into the formulation, Eq. 11 can be rewritten as:

$$M\ddot{d} + C\dot{d} + Kd = F \tag{12}$$

where $\boldsymbol{C}$ is the generalized damping matrix, and it is constructed from $\boldsymbol{K}$ and $\boldsymbol{M}$ with two Rayleigh damping parameters. Newmark time integration algorithm may be utilized to solve Eq. 12, and the mean and standard deviation of response could be directly evaluated by using orthogonal property of Hermite PC. In addition, probability distribution of response is also available by using kernel density estimation with a significant number of generated samples.

3 FORMULATION OF STOCHASTIC DOMAIN REDUCTION METHOD

Conventional approach to simulate seismic wave propagation requires a holistic model including bedrock geology, and local site details (Graves and Pitarka 2010; Rodgers et al. 2018). If the seismic source is far away from the local site, the size of the model would become extremely large and computationally expensive.

Domain reduction method (DRM) (Bielak et al. 2003; Yoshimura et al. 2003), provides a modular, two-step procedure to simulate large scale deterministic seismic wave propagation from far field to local site of interest. The DRM is first used to simulate seismic wave propagation within the deep bedrock, without modelling local site details, and response of boundary layer near the local site is recorded. Note that a coarse mesh can be adopted due high stiffness of the deep bedrock (Lysmer and Kuhlemeyer 1969; Watanabe et al. 2017). Then, a domain reduced model, with local site details is constructed for simulating local site response. Recorded response of the boundary layer from the first step is formulated into effective seismic forces. Those effective seismic forces are then applied on the elements of single boundary layer of the domain-reduced model in a dynamically consistent way. The interior domain Ω, inside the boundary layer, includes all the local site details, while the exterior domain Ω^+ is used to absorb outgoing waves. The key feature of DRM lies in the reduction of computational size to simulate earthquake seismic wave propagation response including local site details. In addition, changes of local site features would only require repeated simulations in its second step and that is much more efficient than traditional approach with a holistic model including the whole bedrock geology and local site. Detailed formulation of domain reduction method can be found in Bielak et al. (2003). Formulation of the first step is neglected herein since it is identical to traditional seismic wave propagation analysis. Traditional seismic wave propagation analysis constructs a holistic model which includes bedrock geology and local site, and the model is discretized using finite element which results in a dynamic equilibrium system of equation. In the second step, the domain reduction formulation can be written in matrix-vector form as:

$$\begin{bmatrix} M_{ii}^{\Omega} & M_{ib}^{\Omega} & 0 \\ M_{bi}^{\Omega} & M_{bb}^{\Omega} + M_{bb}^{\Omega^+} & M_{be}^{\Omega^+} \\ 0 & M_{be}^{\Omega^+} & M_{ee}^{\Omega^+} \end{bmatrix} \begin{Bmatrix} \ddot{u}_i \\ \ddot{u}_b \\ \ddot{\omega}_e \end{Bmatrix} + \begin{bmatrix} K_{ii}^{\Omega} & K_{ib}^{\Omega} & 0 \\ K_{bi}^{\Omega} & K_{bb}^{\Omega} + K_{bb}^{\Omega^+} & K_{be}^{\Omega^+} \\ 0 & K_{be}^{\Omega^+} & K_{ee}^{\Omega^+} \end{bmatrix} \begin{Bmatrix} u_i \\ u_b \\ \omega_e \end{Bmatrix} = \begin{Bmatrix} 0 \\ F_b^{eff} \\ F_e^{eff} \end{Bmatrix} \tag{13}$$

where mass matrix M and stiffness matrix K are formulated with its subscripts i, b, e denoting interior domain, boundary layer, and exterior domain, respectively. Likewise, u_i, u_b and $\ddot{u}_i$, $\ddot{u}_b$ are nodal displacement and acceleration at interior domain, boundary layer, respectively. The residual response w_e in exterior domain is formulated using transformation of variables (Bielak et al. 2003). The effective forces F_b^{eff} and F_e^{eff} are computed from the response of boundary layer elements in the first step, and can be written as:

$$\begin{aligned} F_b^{eff} &= -M_{be}^{\Omega^+} \ddot{u}_e^0 - K_{be}^{\Omega^+} u_e^0 \\ F_e^{eff} &= \quad M_{eb}^{\Omega^+} \ddot{u}_b^0 + K_{eb}^{\Omega^+} u_b^0 \end{aligned} \tag{14}$$

where the superscript "0" denotes the nodal responses collected from simulation in the first step.

Inspired by deterministic domain reduction method, a two-step modular methodology for time-domain stochastic seismic wave propagation is formulated herein. In addition to the spatial separation of exterior domain and interior domain, random field of the two domains are also probabilistically separated into exterior domain random field and interior domain random field. Similar to domain reduction method, the first step is a time-domain intrusive stochastic seismic wave propagation analysis with exterior domain modelled as a non-Gaussian random field, however in the first step, the interior domain is modeled as deterministic domain. In the second step, interior domain is modelled in detail as a random field, and the recorded stochastic response at boundary layer in the first step is applied as stochastic excitations.

Substituting the Hermite PC representation of material parameter, external forcing, response processes (Eq. 2, 7, 8, 9) into Eq. 13, we obtain:

$$
\begin{aligned}
&\sum_{k=1}^{P_3} \Psi_k \begin{bmatrix} M_{ii}^{\Omega} & M_{ib}^{\Omega} & 0 \\ M_{bi}^{\Omega} & M_{bb}^{\Omega} + M_{bb}^{\Omega^+} & M_{be}^{\Omega^+} \\ 0 & M_{be}^{\Omega^+} & M_{ee}^{\Omega^+} \end{bmatrix} \begin{Bmatrix} \ddot{d}_{ik} \\ \ddot{d}_{bk} \\ \ddot{\omega}_{ek} \end{Bmatrix} + \\
&\quad \sum_{k=1}^{P_3} \sum_{m=1}^{P_1} \Psi_m \Psi_k a_m(\mathbf{x}) \begin{bmatrix} K_{ii}^{\Omega} & K_{ib}^{\Omega} & 0 \\ K_{bi}^{\Omega} & K_{bb}^{\Omega} + K_{bb}^{\Omega^+} & K_{be}^{\Omega^+} \\ 0 & K_{be}^{\Omega^+} & K_{ee}^{\Omega^+} \end{bmatrix} \begin{Bmatrix} d_{ik} \\ d_{bk} \\ \omega_{ek} \end{Bmatrix} = \sum_{j=1}^{P_2} \Psi_j \begin{Bmatrix} 0 \\ f_{bj}^{eff} \\ f_{ej}^{eff} \end{Bmatrix}
\end{aligned}
\tag{15}
$$

To apply stochastic Galerkin projection, we multiply a Hermite PC Ψ_l, on both sides. An ensemble average of the equations can then be taken, so that expanded linear system of equations can be formulated as:

$$\sum_{k=1}^{P_3}\langle\Psi_k\Psi_l\rangle \begin{bmatrix} M_{ii}^{\Omega} & M_{ib}^{\Omega} & 0 \\ M_{bi}^{\Omega} & M_{bb}^{\Omega}+M_{bb}^{\Omega^+} & M_{be}^{\Omega^+} \\ 0 & M_{be}^{\Omega^+} & M_{ee}^{\Omega^+} \end{bmatrix} \begin{Bmatrix} \ddot{d}_{ik} \\ \ddot{d}_{bk} \\ \ddot{\omega}_{ek} \end{Bmatrix} +$$

$$\sum_{k=1}^{P_3}\sum_{m=1}^{P_1}\langle\Psi_m\Psi_k\Psi_l\rangle a_m(\mathbf{x}) \begin{bmatrix} K_{ii}^{\Omega} & K_{ib}^{\Omega} & 0 \\ K_{bi}^{\Omega} & K_{bb}^{\Omega}+K_{bb}^{\Omega^+} & K_{be}^{\Omega^+} \\ 0 & K_{be}^{\Omega^+} & K_{ee}^{\Omega^+} \end{bmatrix} \begin{Bmatrix} d_{ik} \\ d_{bk} \\ \omega_{ek} \end{Bmatrix} = \sum_{j=1}^{P_2}\langle\Psi_j\Psi_l\rangle \begin{Bmatrix} 0 \\ f_{bj}^{eff} \\ f_{ej}^{eff} \end{Bmatrix} \tag{16}$$

Similar as in Eq. 13, we can assemble the linear system of equations, Eq. 16, into its matrix-vector form:

$$\begin{bmatrix} \boldsymbol{M}_{ii}^{\Omega} & \boldsymbol{M}_{ib}^{\Omega} & 0 \\ \boldsymbol{M}_{bi}^{\Omega} & \boldsymbol{M}_{bb}^{\Omega}+\boldsymbol{M}_{bb}^{\Omega^+} & \boldsymbol{M}_{be}^{\Omega^+} \\ 0 & \boldsymbol{M}_{be}^{\Omega^+} & \boldsymbol{M}_{ee}^{\Omega^+} \end{bmatrix} \begin{Bmatrix} \ddot{\boldsymbol{d}}_{i} \\ \ddot{\boldsymbol{d}}_{b} \\ \ddot{\boldsymbol{\omega}}_{e} \end{Bmatrix} + \begin{bmatrix} \boldsymbol{K}_{ii}^{\Omega} & \boldsymbol{K}_{ib}^{\Omega} & 0 \\ \boldsymbol{K}_{bi}^{\Omega} & \boldsymbol{K}_{bb}^{\Omega}+\boldsymbol{K}_{bb}^{\Omega^+} & \boldsymbol{K}_{be}^{\Omega^+} \\ 0 & \boldsymbol{K}_{be}^{\Omega^+} & \boldsymbol{K}_{ee}^{\Omega^+} \end{bmatrix} \begin{Bmatrix} \boldsymbol{d}_{i} \\ \boldsymbol{d}_{b} \\ \boldsymbol{\omega}_{e} \end{Bmatrix} = \begin{Bmatrix} \boldsymbol{0} \\ \boldsymbol{F}_{b}^{eff} \\ \boldsymbol{F}_{e}^{eff} \end{Bmatrix} \tag{17}$$

where boldface matrices and vectors indicate the expanded stochastic matrices and vectors from the assembly procedure. The content of stochastic matrices, $\boldsymbol{M}_{ii}^{\Omega}$, $\boldsymbol{K}_{ii}^{\Omega}$, and vectors, $\boldsymbol{d}_i$, $\boldsymbol{F}_b^{eff}$ in Eq. 17 are explicitly written in Equations 18 to 21 to illustrate the assembly procedure,

$$\boldsymbol{M}_{ii}^{\Omega} = \begin{bmatrix} \langle\Psi_1\Psi_1\rangle M_{ii}^{\Omega} & \dots & \langle\Psi_1\Psi_{P_3}\rangle M_{ii}^{\Omega} \\ \vdots & \ddots & \vdots \\ \langle\Psi_{P_3}\Psi_1\rangle M_{ii}^{\Omega} & \dots & \langle\Psi_{P_3}\Psi_{P_3}\rangle M_{ii}^{\Omega} \end{bmatrix} \tag{18}$$

$$\boldsymbol{K}_{ii}^{\Omega} = \begin{bmatrix} \sum_{m=1}^{P_1} \langle \Psi_m \Psi_1 \Psi_1 \rangle a_m(\mathbf{x}) K_{ii}^{\Omega} & \dots & \sum_{m=1}^{P_1} \langle \Psi_m \Psi_1 \Psi_{P_3} \rangle a_m(\mathbf{x}) K_{ii}^{\Omega} \\ \vdots & \ddots & \vdots \\ \sum_{m=1}^{P_1} \langle \Psi_m \Psi_{P_3} \Psi_1 \rangle a_m(\mathbf{x}) K_{ii}^{\Omega} & \dots & \sum_{m=1}^{P_1} \langle \Psi_m \Psi_{P_3} \Psi_{P_3} \rangle a_m(\mathbf{x}) K_{ii}^{\Omega} \end{bmatrix} \tag{19}$$

$$\boldsymbol{d}_i = \begin{bmatrix} d_{i1} \\ \vdots \\ d_{iP_3} \end{bmatrix} \tag{20}$$

$$\boldsymbol{F}_b^{eff} = \begin{bmatrix} \sum_{j=1}^{P_2} \langle \Psi_j \Psi_1 \rangle f_{bj}^{eff} \\ \vdots \\ \sum_{j=1}^{P_2} \langle \Psi_j \Psi_{P_3} \rangle f_{bj}^{eff} \end{bmatrix} \tag{21}$$

while other matrices and vectors in Eq. 17 are assembled in a similar fashion. Size of the stochastic matrix and vector is the size of its corresponding deterministic matrix and vector multiplied by the number of PC coefficients, P_3. The expanded stochastic effective forcing vector can also be computed following Eq. 22, which is the expanded form of Eq. 14,

$$\begin{aligned} \boldsymbol{F}_b^{eff} &= -\boldsymbol{M}_{be}^{\Omega^+} \ddot{\boldsymbol{d}}_e^0 - \boldsymbol{K}_{be}^{\Omega^+} \boldsymbol{d}_e^0 \\ \boldsymbol{F}_e^{eff} &= \boldsymbol{M}_{eb}^{\Omega^+} \ddot{\boldsymbol{d}}_b^0 + \boldsymbol{K}_{eb}^{\Omega^+} \boldsymbol{d}_b^0 \end{aligned} \tag{22}$$

where $\ddot{\boldsymbol{d}}_e^0, \ddot{\boldsymbol{d}}_b^0, \boldsymbol{d}_e^0, \boldsymbol{d}_b^0$ represents the simulated stochastic acceleration and displacement response vectors at the boundary layer in the first step. The expanded matrix-vector form system equations, Eq. 17, can be solved using Newmark time integration scheme. The formulation can also include viscous damping in the system, following Eq. 12. In addition, the proposed modular methodology may be also applicable to other type of interactions between two domains, e.g., hydro-mechanically coupled systems.

4 DEVELOPMENT OF THE STOCHASTIC BEDROCK INPUT MOTIONS

To formulate stochastic effective forces using the above stochastic DRM, it is required to develop stochastic bedrock input motions. For a given site, several different ways have been proposed, e.g., DRM forces can be computed from physics-based simulated ground motions over regional bedrock geology (Graves et al. 2011; Wang et al. 2017; Abell et al. 2018). However, these physics-based ground motion simulations can become computationally intractable when uncertainties in seismic source or bedrock geology need to be considered. For engineering practices, time domain uncertain input motions can be simulated using the stochastic method (Boore 2003). For example, Wang et al. (2020) proposed a methodology to simulate scenario-consistent time domain uncertain motions using stochastic Fourier amplitude spectra and Fourier phase derivative. It is also common practice to scale and select past-recorded seismic motions as the population of underlying uncertain seismic input by matching site-specific target spectrum.

This paper utilizes the PEER online tool to select realistic ground motions by matching site-specific uniform hazard spectrum (UHS) (McGuire 1995) for hazard level of 10% probability of exceedance in 50 years for a target site latitude 34.5°, longitude -118.2° in Los Angeles. Note that the proposed formulation is not only limited to stochastic motions generated from spectrum matching criteria, any stationary or nonstationary seismic motions can be incorporated. Two hundred past-recorded ground motions are selected from PEER online database and scaled for spectral matching. All motions are deconvoluted to the bottom of the bedrock model shown in the next section. The two hundred deconvoluted seismic motions are regarded as realizations of the non-stationary bedrock input random process motions. Figure 1 shows the time series of realizations and the mean response of the random process motions. It is observed that the mean of acceleration is relatively small compared to motion realizations, which is probably due to random phase property of seismic motion.

Marginal mean, standard deviation and correlation structure of the seismic motion random process can be characterized through statistical analysis of these two hundred time series realizations. From the Kolmogorov-Smirnov test of these realizations, it is also found that the marginal distri-

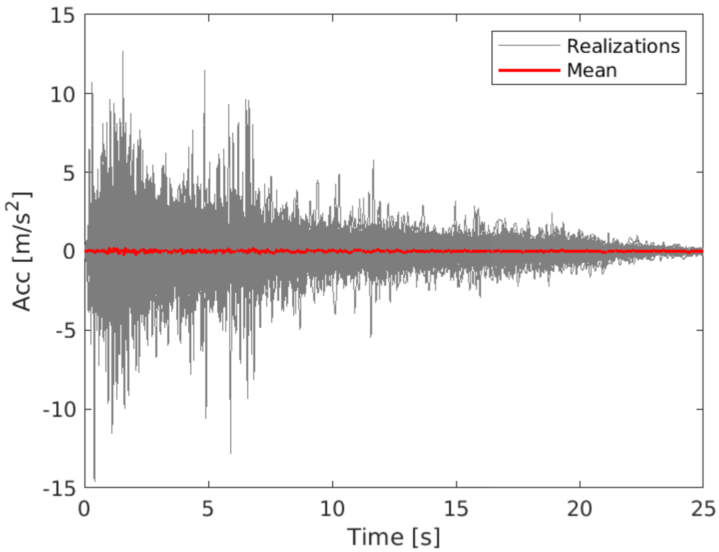

Fig. 1. Time series realizations of the input bedrock random process motions

bution of the seismic motion random process is Gaussian. Therefore, the input stochastic motions are modelled as a non-stationary Gaussian random process and Hermite PC with order 1, that is sufficient to capture the marginal distribution. Hermite polynomial chaos (PC) Karhunen-Loève (KL) expansion, formulated in section 2, is performed to represent such a non-stationary Gaussian random process. Since the seismic random process is highly non-stationary, Hermite PC with dimension 150 is required to sufficiently capture the non-stationary statistics of the random process motions. Figure 2 verifies the correctness of Hermite PC-KL expansion. It can be seen that both marginal mean and standard deviation synthesized from Hermite PC representation are close to the statistics derived from the realizations of seismic motions.

In addition to the marginal behaviour, Hermite PC-KL representation can also reproduce the correlation structure of the seismic motion random process, as shown in Figure 3. The PC represented random process motions would be used as uncertain bedrock input in the illustrative examples 2 and 3 in the next section.

5 ILLUSTRATIVE EXAMPLES

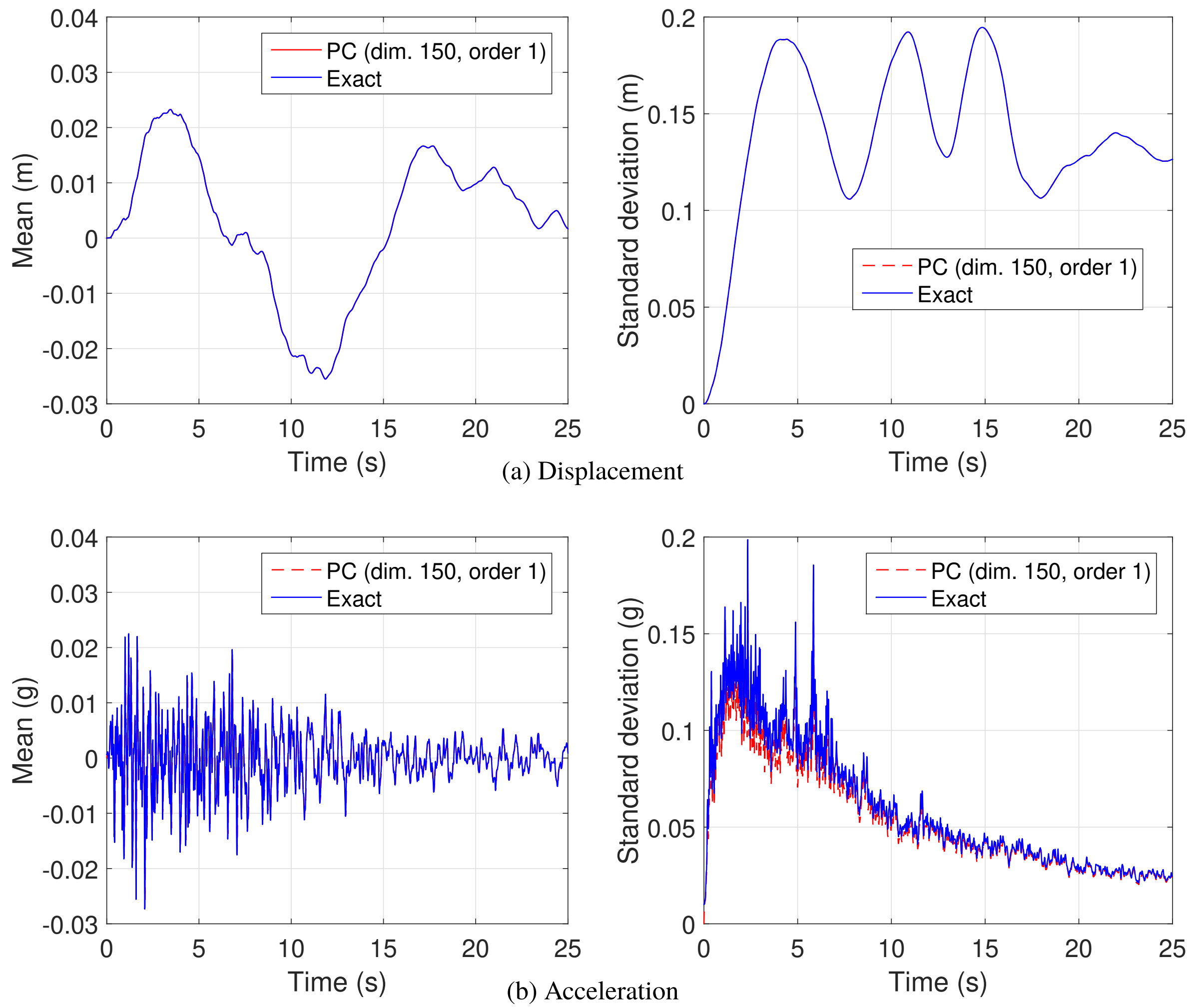

(a) Displacement

(b) Acceleration

Fig. 2. Marginal mean and standard deviation responses of the non-stationary input motion random process: (a) Displacement, and (b) Acceleration.

In order to illustrate the proposed modular approach, 1-D seismic wave propagation analysis for an engineering site is performed. The site is located at latitude 34.5°, longitude -118.2° in Los Angeles with 280m thick bedrock and 20m thick overlying soil. Input seismic excitations are applied at the bottom of the bedrock. Three examples are presented in this section. The first example considers uncertain ground shear modulus only. The second example considers uncertain seismic motions only, while the third example considers uncertainties in both input motions and material. In addition, conventional holistic stochastic seismic wave propagation analysis is also conducted for verification. A schematic illustration of the conventional holistic model is shown in

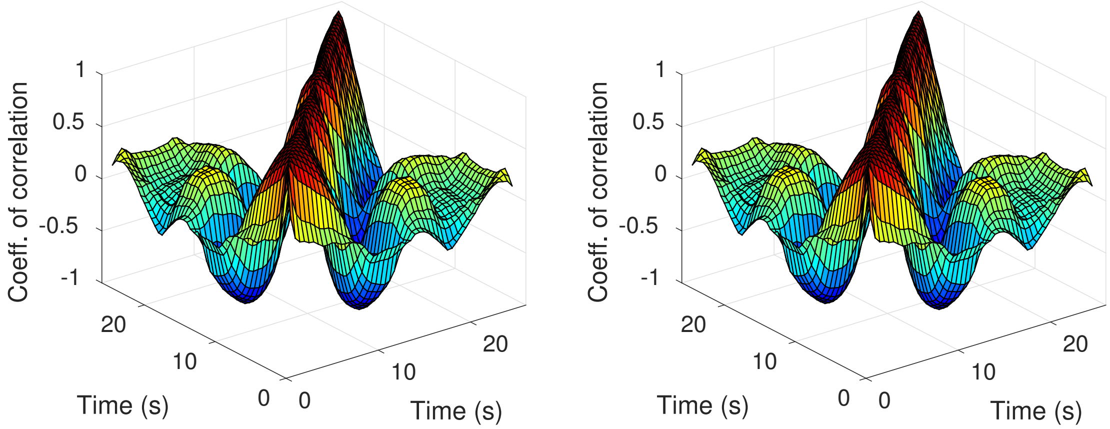

(a) Exact **(b)** PC Synthesized

Fig. 3. Correlation structure of the non-stationary input motion random process: (a) Exact (b) PC Synthesized.

Figure 4, and the two modular models in the proposed approach are shown in Figure 5.

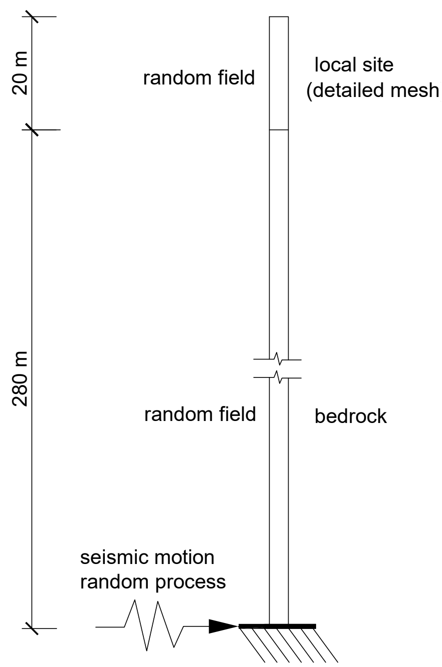

Fig. 4. Holistic 1-D stochastic seismic wave propagation model using conventional approach.

Boundary layer should be located a distance away from local site with Dashpot at the bottom to absorb outgoing waves and avoid wave reflection. In order to determine a reasonable location

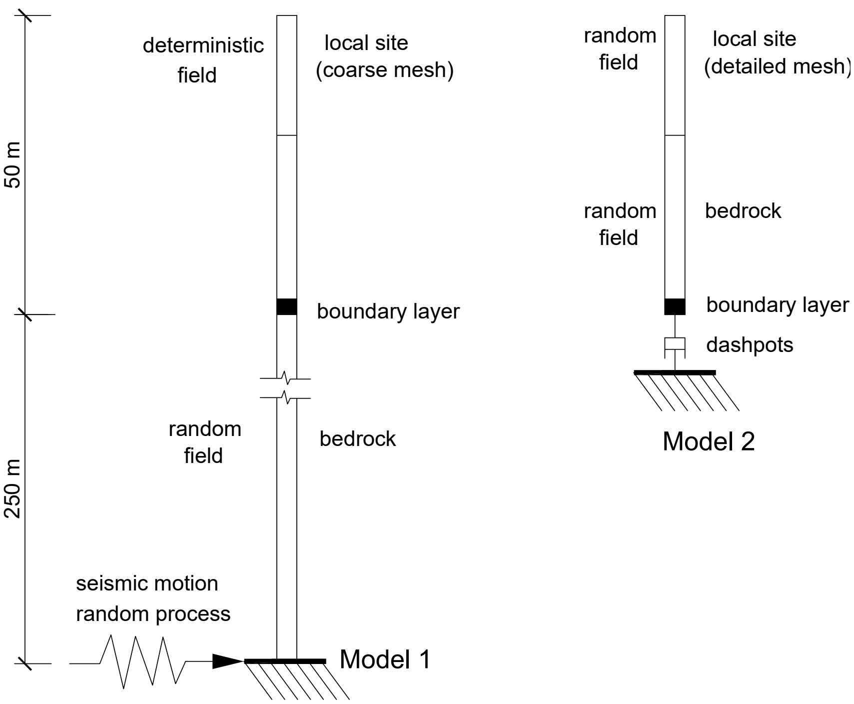

Fig. 5. 1-D stochastic seismic wave propagation model using modular approach: (a) Model 1 in the first step; (b) Model 2 in the second step

of boundary layer, analyses with different distances to local site (10m, 20m, 30m) are performed. We found that for boundary layer located at 30m from the local site, good agreement with results from conventional approach is achieved, and the reflected waves at the boundary layer are mostly absorbed and residual waves are negligible Therefore, 30m to the local site is selected for the boundary layer location in the model. Noted that procedures to determine the boundary layer location is dependent on geology and it is recommended that numerical tests be performed in order to gain confidence in model geometry. In other words, analysts are encouraged to perform model verification in order to determine appropriate dimensions of the model. Note that the proposed modular approach is also applicable to 2-D and 3-D problems, and the employed 1-D model in this paper is to verify the proposed modular formulation.

The uncertain shear modulus of the 20-meter local site is modelled as a homogeneous lognormal random field with marginal mean 100 MPa, coefficient of variation (COV) 30% and exponential correlation structure with correlation length of 5m. Similarly, shear modulus of bedrock is another lognormal random field with marginal mean linearly increasing from top to bottom, 100 MPa to 1000 MPa, COV 20%, exponential correlation structure with correlation length of 100 m. Note that the two shear modulus random fields represent two distinct parts of the model, therefore, they are mutually independent. Simulations in this paper are run using a desktop with Intel Core i7-7700 CPU @ 3.60 Hz processor.

5.1 Example 1: Uncertain shear modulus with deterministic input motion

We use Hermite PC with dimension 3, order 2 to quantify the lognormal random field of shear modulus of local site, and another Hermite PC of dimension 3 order 2 for the lognormal random field of shear modulus of bedrock. Since the two random fields are mutually independent, Hermite PC with dimension 6 order 2 should be used for the stochastic response. The input deterministic seismic motion, as shown in Figure 6, is the deconvoluted ground motion recorded at Devil's canyon station of 1970 Lytle Creek Earthquake, that is selected by spectrally matching the site-specific design spectrum.

Rayleigh damping ratio of 5% is used and the two Rayleigh parameters are computed by assigning 5% damping to the first and fourth natural frequencies of the site profile with no uncertainties (0.46 Hz, 2.6 Hz). By analyzing the natural frequencies with 1000 realizations of site profile, the damping ratio for the extreme case (the first natural frequency 0.23Hz) is 8.5% that is a bit higher than 5%. Therefore, the Rayleigh parameters that were used in modeling yield approximately 5% damping ratio in major modes and thus avoid unrealistic large damping ratios even for the extreme cases of site profile realizations.

Figure 7 shows the simulated marginal mean and standard deviation of displacement and acceleration at the ground surface from both the conventional holistic approach and the proposed modular approach. Peaks of mean and standard deviation of displacement are 0.03m and 0.012m, respectively. The COV of ground displacement is approximately 40%, which is larger than input COV (30%) of shear modulus. Similarly, COV of ground acceleration is approximately 2 since peaks of mean and standard deviation of acceleration are 0.15g and 0.3g, respectively. Although the COV of input shear modulus is only 30%, COV of ground acceleration is nearly 2, and that is

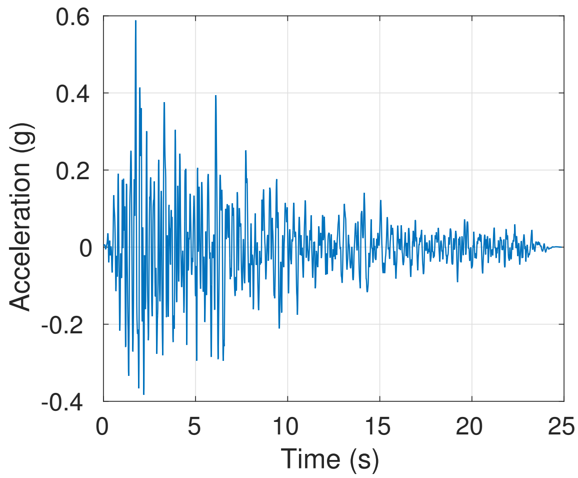

Fig. 6. Time history of of the deterministic bedrock input motion

quite unexpected from engineering judgment point of view. It can be seen that marginal mean and standard deviation of ground response from the proposed modular approach are in good agreement with results from the conventional holistic approach. Only slight difference is observed in the marginal standard deviation of acceleration at ground surface.

The solved Hermite PC expansion of ground surface displacement at time 8.0 s is shown in Eq. 23. The Hermite PC expansion is dimension 6 order 2 with 28 PC coefficients, and the first seven PC terms are presented in Eq. 23 due to space limitation. It is observed that the first four PC coefficients from the modular approach agrees very well with those from the conventional approach.

$$\begin{aligned} d_{con}(t = 8.0s) = &\quad (-58 - 7.87\xi_1 - 2.99\xi_2 + 1.90\xi_3 + 0.61\xi_4 + 0.03\xi_5 + 0.02\xi_6) \times 10^{-4} \\ d_{mod}(t = 8.0s) = &\quad (-57 - 7.39\xi_1 - 3.08\xi_2 + 1.99\xi_3 - 1.24\xi_4 - 0.96\xi_5 - 0.19\xi_6) \times 10^{-4} \end{aligned} \tag{23}$$

In addition, the marginal probabilistic density function (PDF) of uncertain ground surface displacement at time 8.0 s is estimated by kernel density approach as shown in Figure 8. It is observed that the marginal PDF of ground displacement from the modular approach also matches well with the PDF from the conventional holistic approach, but shifts slightly to the right. The conventional approach takes 9.7 seconds while the modular approach takes 3.1 seconds.

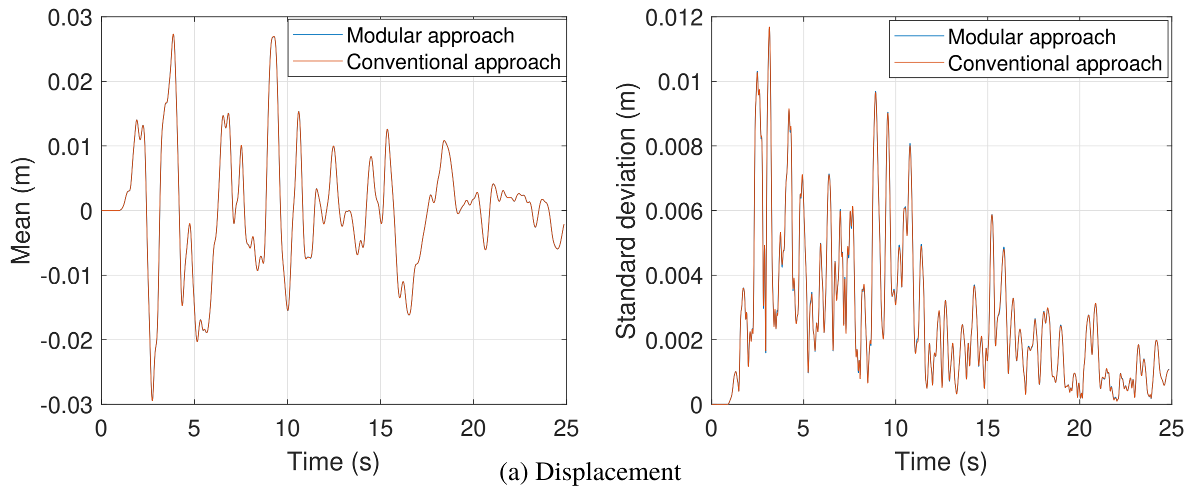

(a) Displacement

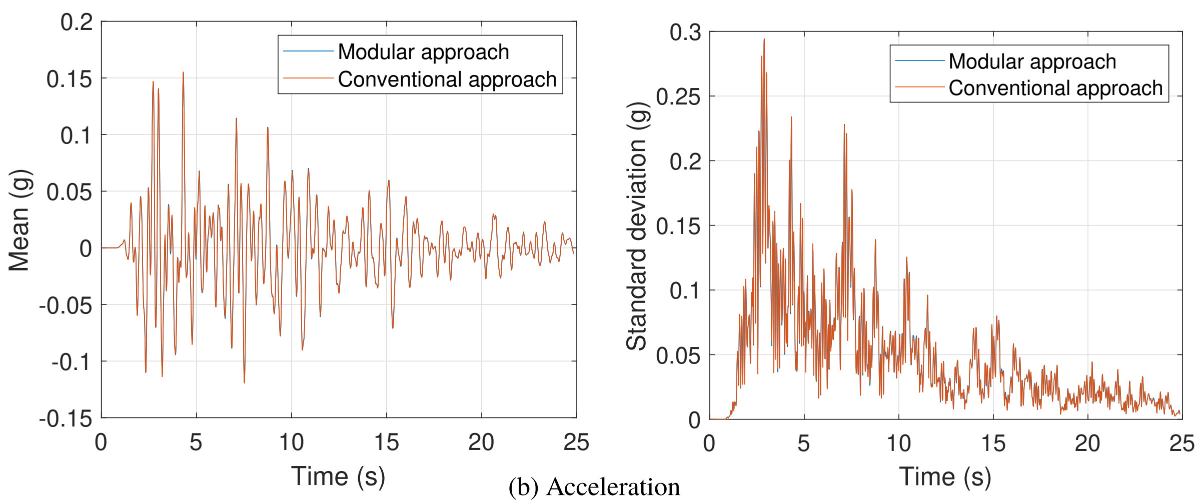

(b) Acceleration

Fig. 7. Simulated marginal mean and standard deviation of: (a) Displacement, and (b) Acceleration at the ground surface when only shear modulus is uncertain.

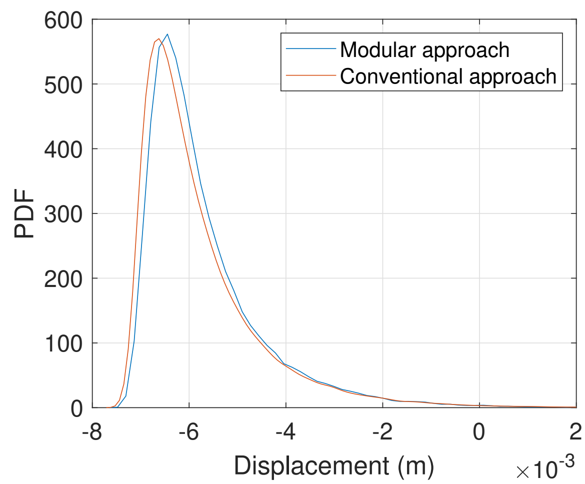

Fig. 8. Simulated marginal PDF of surface displacement at 8.0s when only shear modulus is uncertain.

5.2 Example 2: Deterministic shear modulus with uncertain input motions

In the second example, we keep the shear modulus of the ground as deterministic and input the stochastic seismic motions presented in section 4. Stochastic seismic wave propagation is analyzed using both the conventional holistic approach and the proposed modular approach. Time-evolving marginal mean and standard deviation of surface displacement and acceleration from both approaches are compared in Figure 9.

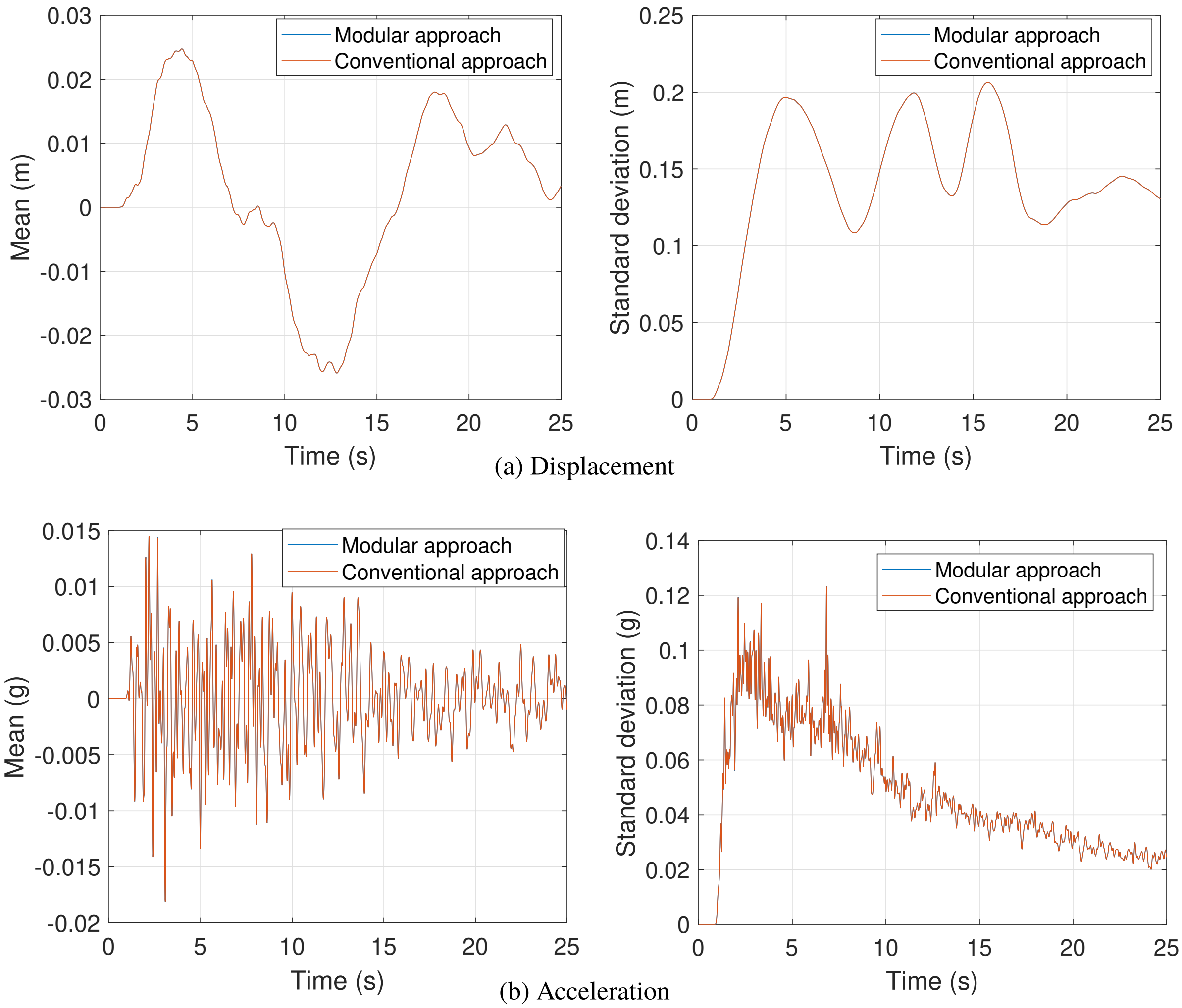

(a) Displacement

(b) Acceleration

Fig. 9. Simulated marginal mean and standard deviation of: (a) Displacement, and (b) Acceleration at the surface when only bedrock input motions are uncertain.

The overlapping responses in Figure 9 confirm the validity of the proposed modular approach. The PDF of probabilistic displacement response at 8.0s is shown in Figure 10. Same as the

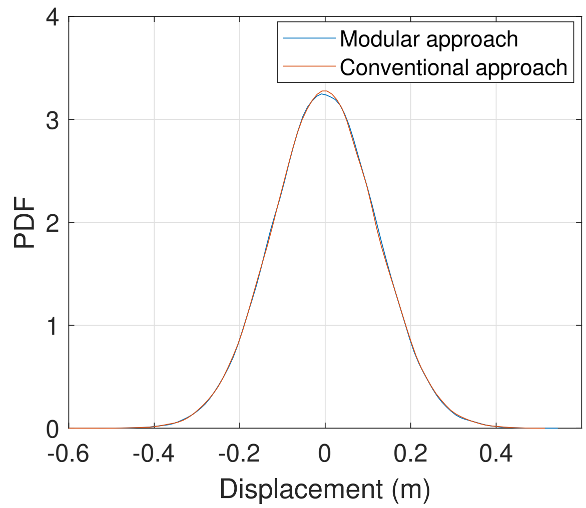

Fig. 10. Simulated marginal PDF of surface displacement at 8.0 s when only bedrock motion is uncertain.

uncertain input motions, it is observed that the standard deviation responses of both displacement and acceleration are much larger than corresponding mean responses. The result from the proposed modular approach is also matching well with that from the conventional holistic approach except for slight difference on the peaks of PDF. The PDF of probabilistic surface displacement shows clear Gaussian nature. This is expected considering the input seismic motion is a non-stationary Gaussian random process and the ground shear modulus is deterministic. In addition, the conventional approach takes 13.1 seconds while the modular approach takes 3.4 seconds.

5.3 Example 3: Uncertain shear modulus with uncertain input motion

The third example considers both the shear modulus and input bedrock motions to be uncertain. The shear modulus random fields of local site and bedrock are identical to Example 1, which is represented by PC dimension 3 order 2 for each random field. The seismic motion random process is identical to Example 2, which is represented by PC dimension 150 order 1. Since two shear modulus random fields and input motion random process are mutually independent, the probabilistic response process is represented by Hermite PC dimension 156 order 2 to encompass the entire probability space.

Figure 11 shows the second-order statistics of displacement and acceleration at the ground surface from stochastic finite element analysis. The marginal PDF of surface displacement at 8.0s

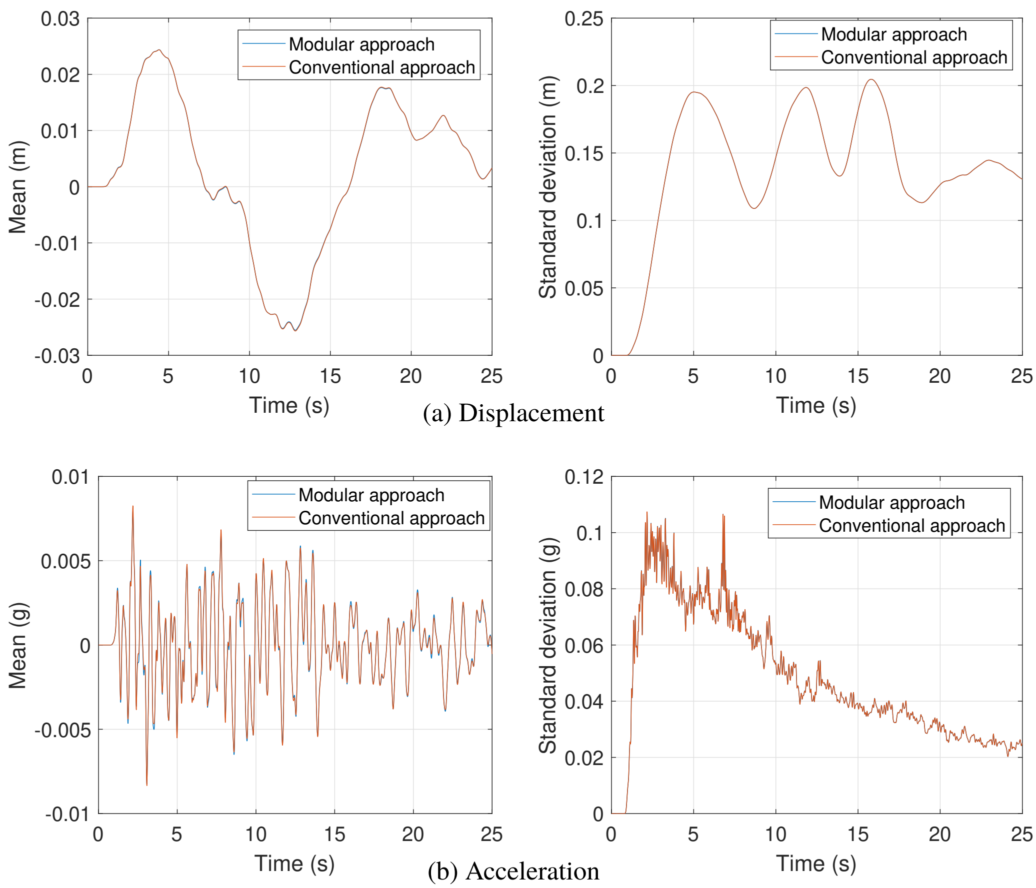

Fig. 11. Simulated marginal mean and standard deviation of: (a) Displacement, (b) Acceleration at the surface when both the shear modulus and input bedrock motions are uncertain.

is shown in Figure 12. Similar to Example 1 and Example 2, good agreement of results from the

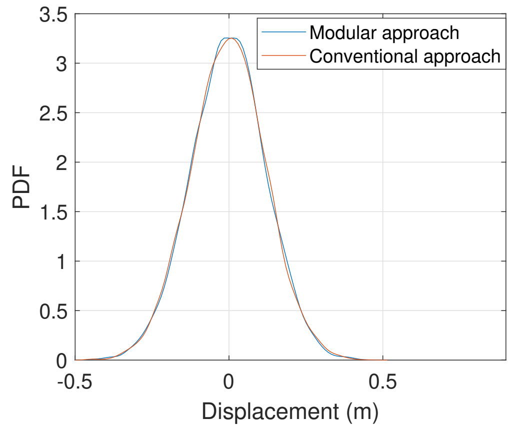

Fig. 12. Simulated marginal PDF of surface displacement at 8.0 s when both shear modulus and input bedrock motions are uncertain.

proposed modular approach and conventional holistic approach is observed for both time-evolving marginal mean, standard deviation and PDF of probabilistic surface response. It is also noted that the magnitude and shape of mean and standard deviation of ground surface response are close to those of uncertain input motions. This implies that the probabilistic system response from the stochastic wave propagation is dominantly controlled by the uncertain input excitations. This is confirmed by Figure 13 where probabilistic surface acceleration responses from example 2 (uncertain motion) and example 3 (uncertain motion & modulus) are compared. It can be seen that introducing shear modulus uncertainty (20% COV) to the system with uncertain input motions would not make significant difference to the surface probabilistic response. There is some decrease in the mean acceleration response after incorporating modulus uncertainty. However, its influence is very small considering that the magnitude of standard deviation is much larger than the mean response. In addition, the conventional approach takes 3844.2 seconds while the modular approach takes 1010.6 seconds. Taking the simulation time in all three examples into account, the proposed modular approach is more than three times faster than the conventional approach.

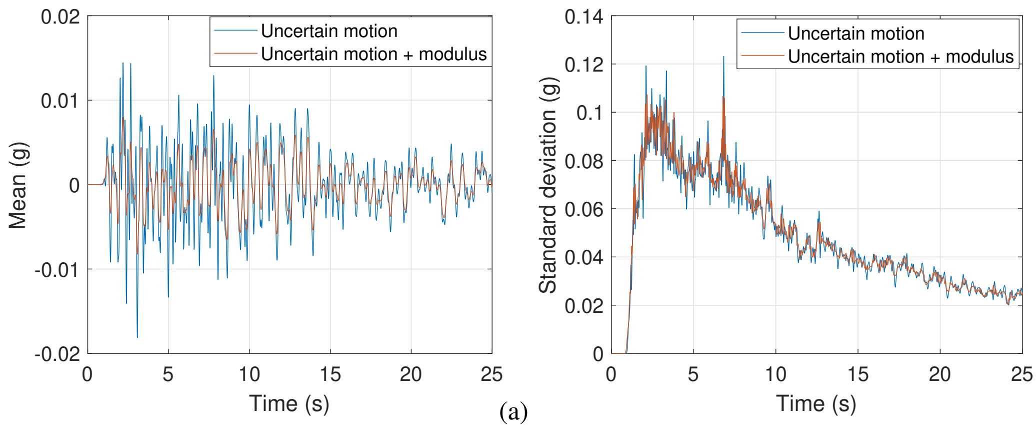

(a)

Fig. 13. Simulated marginal mean and standard deviation of acceleration at ground surface: Comparison of example 2 (uncertain motion) and example 3 (uncertain motion + modulus).

6 CONCLUSIONS

In this paper, a modular methodology is developed for time-domain intrusive stochastic modelling of non-stationary seismic wave propagation from bedrock to local site through inhomogeneous random medium. Hermite polynomial chaos expansion is employed to quantify the uncertain material parameters and uncertain seismic motion. Uncertain seismic motions, resulting from uncertain input motions, are intrusively propagated through the uncertain material using Galerkin stochastic finite element method. The Hermite polynomial chaos expansion is capable of simulating any non-Gaussian and non-stationary random process or field. By formulating stochastic effective seismic input forces, conventional deterministic domain reduction method is mathematically extended to probabilistic regime. The novelty of the proposed methodology lies in the two-step modular approach to propagating uncertain motions, from uncertain input through uncertain material. The first step performs a stochastic wave propagation from random process input motions, through a detailed random field model of bedrock and a coarse deterministic local site model. The second step then involves stochastic simulation of a reduced domain containing detailed random field model of a local site, excited by uncertain effective forces developed using motions from the first step. Compared to the conventional holistic approach for stochastic seismic wave propagation, simulated domain in both steps is reduced and computationally tractable. The separation of uncertain local site from uncertain deep bedrock model is more practical since it enables efficient simulation with frequent modification and parametric study of local site conditions.

A 1-D seismic wave propagation analysis with three cases is used to verify and illustrate the proposed methodology. Results show that simulated mean, standard deviation, and PDF of ground response is in good agreement with those from the conventional holistic approach. The proposed modular methodology offers a more efficient and practical approach to simulate stochastic seismic wave propagation. In addition, for 3D problems, developed methodology will provide even more efficiencies for stochastic seismic wave propagation modelling.

ACKNOWLEDGMENT

The work presented in this paper was supported in part by the United States Department of

Energy.

REFERENCES

Abell, J. A., Orbović, N., McCallen, D. B., and Jeremić, B. (2018). “Earthquake soil structure interaction of nuclear power plants, differences in response to 3-D, 3×1-D, and 1-D excitations.” *Earthquake Engineering and Structural Dynamics*, 47(6), 1478–1495.

Babuška, I., Nobile, F., and Tempone, R. (2007). “A stochastic collocation method for elliptic partial differential equations with random input data.” *SIAM Journal on Numerical Analysis*, 45(3), 1005–1034.

Bathe, K.-J. (1996). *Finite Element Procedures in Engineering Analysis*. Prentice Hall Inc. ISBN 0-13-301458-4.

Berveiller, M., Sudret, B., and Lemaire, M. (2006). “Stochastic finite element: A non-intrusive approach by regression.” *European Journal of Computational Mechanics*, 15, 81–92.

Bielak, J., Loukakis, K., Hisada, Y., and Yoshimura, C. (2003). “Domain reduction method for three–dimensional earthquake modeling in localized regions. part I: Theory.” *Bulletin of the Seismological Society of America*, 93(2), 817–824.

Boore, D. M. (2003). “Simulation of ground motion using the stochastic method.” *Pure and Applied Geophysics*, 160, 635–676.

Bourret, R. C. (1962). “Propagation of randomly perturbed fields.” *Canadian Journal of Physics*, 40, 782–790.

Fenton, G. A. and Griffiths, D. V. (2002). “Probabilistic foundation settlement on spatially random soil.” *Journal of Geotechnical and Geoenvironmental Engineering, ASCE*, 128(5), 381–390.

Fenton, G. A. and Griffiths, D. V. (2005). “Three-dimensional probabilistic foundation settlement.” *ASCE Journal of Geotechnical and Geoenvironmental Engineering*, 131(2), 232–239.

Ghanem, R. G. and Spanos, P. D. (1991). *Stochastic Finite Elements, A Spectral Approach*. Dover Publications Inc., revised edition edition.

Graves, R., Jordan, T., Callaghan, S., Deelman, E., Field, E., Juve, G., Kesselman, C., Maechling, P., Mehta, G., Milner, K., Okaya, D., Small, P., and Vahi, K. (2011). "Cybershake: A physics-based seismic hazard model for southern california." *Pure and Applied Geophysics*, 168(3), 367–381.

Graves, R. W. and Pitarka, A. (2010). "Broadband ground-motion simulation using a hybrid approach." *Bulletin of the Seismological Society of America*, 100(5A), 2095–2123.

Isbiliroglu, Y., Taborda, R., and Bielak, J. (2015). "Coupled soil-structure interaction effects of building clusters during earthquakes." *Earthquake Spectra*, 31(1), 463–500.

Jeremić, B., Jie, G., and Preisig, M. (2007). "Benefits and detriments of soil foundation structure interaction." *GeoDenver*.

Jeremić, B., Jie, G., Preisig, M., and Tafazzoli, N. (2009). "Time domain simulation of soil–foundation–structure interaction in non–uniform soils.." *Earthquake Engineering and Structural Dynamics*, 38(5), 699–718.

Jeremić, B. and Preisig., M. (2005). "Seismic soil–foundation–structure interaction: Numerical modeling issues.." *ASCE Structures Congress*, New York, NY, U.S.A. (April 20-24).

Jeremić, B., Yang, Z., Cheng, Z., Jie, G., Tafazzoli, N., Preisig, M., Tasiopoulou, P., Pisanò, F., Abell, J., Watanabe, K., Feng, Y., Sinha, S. K., Behbehani, F., Yang, H., and Wang, H. (1989-2021). *Nonlinear Finite Elements: Modeling and Simulation of Earthquakes, Soils, Structures and their Interaction*. Self Published, University of California, Davis, CA, USA URL: http://sokocalo.engr.ucdavis.edu/~jeremic/LectureNotes/.

Kausel, E. (1994). "Thin-layer method: Formulation in time domain." *International Journal for Numerical Methods in Engineering*, 37, 927–941.

Kontoe, S., Zdravković, L., and Potts, D. M. (2009). "An assessment of the domain reduction method as an advanced boundary condition and some pitfalls in the use of conventional absorbing boundaries." *International Journal for Numerical and Analytical Methods in Geomechanics*, 33(3), 309–330.

Liu, J., Du, Y., Du, X., Wang, Z., and Wu, J. (2006). "3D viscous-spring artificial boundary in time domain." *Earthquake Engineering and Engineering Vibration*, 5(1), 93–102.

Lysmer, J. and Kuhlemeyer, R. L. (1969). "Finite dynamic model for infinite media." *Journal of*

Engineering Mechanics Division, ASCE, 95(EM4), 859–877.

Lysmer, J. and Waas, G. (1972). "Shear waves in plane infinite structures." *Journal of the Engineering Mechanics Division*, 98(1), 85–105.

Manolis, G. D. and Shaw, R. P. (1996). "Harmonic wave propagation through viscoelastic heterogeneous media exhibiting mild stochasticity: I. Fundamental solution." *Soil Dynamic and Earthquake Engineering*, 15, 119–127.

McGuire, R. K. (1995). "Probabilistic seismic hazard analysis and design earthquakes: closing the loop." *Bulletin of the Seismological Society of America*, 85(5), 1275–1284.

Metropolis, N. and Ulam, S. (1949). "The Monte Carlo method." *Journal of the American Statistical Association*, 44(247), 335–341.

Moehle, J. and Deierlein, G. G. (2004). "A framework methodology for performance-based earthquake engineering." *13th world conference on earthquake engineering*, Vol. 679.

Rahman, M. S. and Yeh, C. H. (1996). "Variability of seismic response of soils using stochastic finite element method." *Soil Dynamic and Earthquake Engineering*, 18, 229–245.

Rodgers, A., Pitarka, A., Petersson, N., Sjögreen, B., and McCallen, D. (2018). "Broadband (0-4 hz) ground motions for a magnitude 7.0 Hayward fault earthquake with 3D structure and topography." *Geophys. Res. Lett.*, 45 doi: 10.1002/2017GL076505.

Sakamoto, S. and Ghanem, R. (2002). "Polynomial chaos decomposition for the simulation of non-gaussian nonstationary stochastic processes." *Journal of Engineering Mechanics*, 128(2), 190–201.

Sett, K., Jeremić, B., and Kavvas, M. L. (2011). "Stochastic elastic-plastic finite elements." *Computer Methods in Applied Mechanics and Engineering*, 200(9-12), 997–1007.

Shinozuka, M. (1972). "Monte carlo solution of structural dynamics." *Computers and Structures*, 2, 855–874.

Sudret, B. and Kiureghian, A. D. (2000). "Stochastic finite element methods and reliability: A state–of–the–art report." *Report No. UCB/SEMM-2000/08*, University of California at Berkeley (November).

Wang, F. and Sett, K. (2016). "Time-domain stochastic finite element simulation of uncertain seismic wave propagation through uncertain heterogeneous solids." *Soil Dynamics and Earthquake Engineering*, 88, 369 – 385.

Wang, F. and Sett, K. (2019). "Time domain stochastic finite element simulation towards probabilistic seismic soil-structure interaction analysis." *Soil Dynamics and Earthquake Engineering*, 116, 460 – 475.

Wang, H., Wang, F., Yang, H., Feng, Y., Bayless, J., Abrahamson, N. A., and Jeremić, B. (2020). "Time domain intrusive probabilistic seismic risk analysis of nonlinear shear frame structure." *Soil Dynamics and Earthquake Engineering*, 136, 106201.

Wang, H., Yang, H., Sinha, S. K., Feng, Y., Luo, C., McCallen, D. B., and Jeremić, B. (2017). "3D non-linear earthquake soil-structure interaction modeling of embedded small modular reactor (SMR)." *Proceedings of the 24th International Conference on Structural Mechanics in Reactor Technology (SMiRT 24)*, Busan, South Korea (August 20-25).

Watanabe, K., Pisanò, F., and Jeremić, B. (2017). "Discretization effects in the finite element simulation of seismic waves in elastic and elastic-plastic media." *Engineering with Computers*, 33(3), 519–545.

Xiu, D. (2010). *Numerical Methods for Stochastic Computations*. Princeton University Press.

Xiu, D. and Hesthaven, J. S. (2005). "High-order collocation methods for differential equations with random inputs." *SIAM Journal on Scientific Computing*, 27(3), 1118–1139.

Yoshimura, C., Bielak, J., and Hisada, Y. (2003). "Domain reduction method for three–dimensional earthquake modeling in localized regions. part II: Verification and examples." *Bulletin of the Seismological Society of America*, 93(2), 825–840.

Zhang, R. R. and Lou, M. (2001). "Seismic wave motion modelling with layered 3D random heterogeneous media." *Probabilistic Engineering Mechanics*, 16(4), 381–397.